

**Best  
Available  
Copy**

AD-765 833

CONDUCTION MECHANISMS IN THICK FILM  
MICROCIRCUITS

R. W. Vest

Purdue Research Foundation

Prepared for:

Advanced Research Projects Agency

1 August 1973

DISTRIBUTED BY:

**NTIS**

National Technical Information Service  
U. S. DEPARTMENT OF COMMERCE  
5285 Port Royal Road, Springfield Va. 22151

AD 765833

Semi-annual Technical Report  
for the Period 1/1/73 - 6/30/73

Conduction Mechanisms in Thick  
Film Microcircuits

Grant Number: DAHCl5-70-G7

ARPA Order no.: 1642

Grantee: Purdue Research Foundation

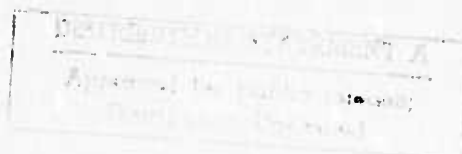
Principal Investigator: R. W. Vest  
(317) 749-2601

Effective Date of Grant: 7/1/70

Grant Expiration Date: 6/30/73

Amount of Grant: \$181,260

August 1, 1973



Reproduced by  
NATIONAL TECHNICAL  
INFORMATION SERVICE  
U.S. Department of Commerce  
Springfield, VA 22151

## Forward

Research described in this report constitutes the sixth six months effort under a grant from the Defense Advance Research Projects Agency, Department of Defense, under the technical cognizance of Dr. Norman Tallan, Aerospace Research Laboratories, U. S. Air Force. The research was conducted in the Turner Laboratory for Electroceramics, School of Electrical Engineering and School of Materials Engineering, Purdue University, West Lafayette, Indiana 47907, under the direction of Professor R. W. Vest. Contributing to the project were Assistant Professor G. L. Fuller, Mr. D. J. Deputy, Mr. E. M. Miller, Mr. A. N. Prabhu, Mr. T. R. Raghunath, Mr. R. L. Reed, and Mr. J. L. Wright.

# 11

## ABSTRACT

The solubility of  $\text{RuO}_2$  in 63%  $\text{PbO}$ -25%  $\text{B}_2\text{O}_3$ -12%  $\text{SiO}_2$  glass has been determined as a function of temperature, both for the equilibrium case and for times typically associated with thick film resistor firing. Studies with the hot stage metallograph have demonstrated the feasibility of obtaining quantitative sintering data with this experimental tool, and have shown the release of gas bubbles from resistors for unexpectedly long periods of time at normal firing temperatures. Possible sources of the escaping gas and the implication as regards the sintering model are discussed. It was demonstrated that no new crystal phases are formed during a normal resistor firing profile, but that crystalline phases originating from an interaction between the glass and the alumina substrate are formed during extended firing periods. Resistor firing studies have demonstrated that the microstructure formation can be successfully slowed by lower temperature operation while still developing the identical ultimate structure. This work allows the structure to be quenched at varying stages of development for subsequent analysis. Studies of resistance during the microstructure development process have led to the conclusion that two different charge transport mechanisms may occur during the firing sequence, and that the relative contributions of these two mechanisms depend upon the particle size and particle size distribution of the conductive phase, as well as the degree of dispersion of the formulation.

## TABLE OF CONTENTS

	<u>Page</u>
I. Introduction	1
II. Microstructure Determination	3
A. $\text{RuO}_2$ Solubility	3
B. Glass Sintering	7
C. $\text{RuO}_2$ Sintering in Glass	8
D. Resistor Firing	10
E. New Phases	16
III. Resistor Firing	20
A. Old Paste	20
B. New Paste	24
C. Conduction Mechanisms	25
IV. Industrial Coupling	34
A. Tunnel Kiln and Profile	35
B. End Member Pastes	42
C. Comparison to Old Paste	42
V. Summary and Future Plans	46
VI. References	49
VII. Distribution List	50

## LIST OF FIGURES

<u>Figure</u>		<u>Page</u>
1	Solubility of Ru in 63% PbO-25% B <sub>2</sub> O <sub>3</sub> -12% SiO <sub>2</sub> Glass	6
2	Successive Stages of Neck Growth During Sintering of Glass Spheres	9
3	RuO <sub>2</sub> Particles in Glass	11
4	Movement of RuO <sub>2</sub> Particles in Glass	12
5	Resistor Surface at 700°C Showing Gas Bubble Density	14
6	Resistor Network Development	15
7	Crystalline Structures Formed During Resistor Firing	17
8	Resistance and TCR versus Firing Time for 640°C Maximum Temperature	21
9	Resistor Macrostructure Development at 640°C (40X)	23
10	Resistance versus Firing Time for 610°C Maximum Temperature	26
11	TCR versus Firing Time for 610°C Maximum Temperature	27
12	Normalized Resistance for Various Firing Times at 630°C	28
13	Resistance Changes During Firing From 513°C to 625°C	31
14	Dried Resistors Prior to Firing	32
15	Lindberg Tunnel Kiln	36
16	Tunnel Kiln Schematic	37
17	Tunnel Kiln Temperature Gradient	39
18	Standard Time-Temperature Profile	40
19	Resistance versus Belt Speed	41
20	Rheological Properties of Resistor Pastes	43

## 1. Introduction

Advances in thick film technology have been hindered by an inadequate understanding of the relationships between the physical properties of the ingredient materials and the electrical properties of the resulting resistors and conductors. The lack of a predicted model of the conduction mechanism has hampered the development of new materials, as well as the improvement of existing systems. The two primary concerns of the present research program in the area of resistor technology are the development of adequate models to describe the "Blending Curve Anomaly" and the "TCR Anomaly." The "Blending Curve Anomaly" refers to the often reported observation that with oxidic conductors and glass the sheet resistance varies monotonically from very low (e.g. 1 V/O) to very high conductive concentrations; whereas, with noble metal conductives and glass electrical continuity is not achieved until the amount of conductive approaches 50 V/O. The primary scientific question is: what are the driving forces which are responsible for the formation of continuous conducting paths along the length of the resistor at such low concentrations of the conductive? The "TCR Anomaly" refers to the fact the temperature coefficient of resistance of a resistor is much lower than the TCR of any of the individual ingredients from which it was made. The primary scientific question is: what is the mechanism by which electric charge is transported?

The primary thrust of the experimental program is to relate electrical properties of the thick films to the materials properties and processing conditions through microstructure. The materials properties to be correlated are: resistivity, temperature coefficient of resistivity, coefficient of thermal expansion, interfacial energy, particle shape, size and size



distribution, and chemical reactivity with other constituents. The processing conditions to be correlated are time, temperature and atmosphere during firing. The specific objectives of the program are:

1. Determine the dominant sintering mechanisms responsible for microstructure development and establish the relative importance of the various properties of the ingredient materials.
2. Determine the dominant mechanisms limiting electrical charge transport, and establish the relative importance of the various properties of the ingredient materials.
3. Develop phenomenological models to interrelate the various materials properties with systems performance.

The majority of the work described in this report was directed toward objectives 1 and 3 above. Earlier reports [1-5] dealt with objective 2, in addition to 1 and 3, and additional studies in progress will be discussed at a later time.

## II. Microstructure Determination

The microstructure of the fixed resistor is directly related to its electrical properties and thus must be determined in order to establish better control of critical resistor fabrication steps. Early experiments with the resistor system being studied in this project ( $\text{RuO}_2$ -lead borosilicate glass) were limited to electrical measurements which determined limits on possible microstructure parameters and permitted more accurate speculation as to possible reactions occurring during firing. These types of measurements have continued and remain a valuable technique. More recently, this work has been supplemented with optical and SEM photomicrographs. During the present reporting period, several experiments have been initiated and/or completed that are direct measurements of microstructure development parameters. These are:  $\text{RuO}_2$  solubility in glass, glass sintering,  $\text{RuO}_2$  sintering, the firing of  $\text{RuO}_2$ -glass composites, including resistors, and the detection of new phases. Quantitative information on these reactions or parameters is necessary to properly verify the proposed microstructure model [6]. Many of the experiments reported here were done with the hot stage video metallograph described earlier [7].

### A. $\text{RuO}_2$ Solubility

The microstructure development model has, as one of its sequential steps, the sintering of the  $\text{RuO}_2$  in the presence of glass. In order to quantify this reaction in the model, it is necessary to determine the types of sintering that take place during resistor firing. A possible mechanism would be solution-dissolution in which  $\text{RuO}_2$  would dissolve at the particle surfaces with a convex radius of curvature, diffuse through the glass, and

reprecipitate at the concave radius of curvature in the neck region being formed; the driving force, as in any sintering process, being a reduction in total surface area. Earlier experiments [8] indicated that the solubility of  $\text{RuO}_2$  in the lead borosilicate glass is low, e.g.  $\leq 200$  ppm, for temperatures up to  $900^\circ\text{C}$ . The only other known solubility measurements for  $\text{RuO}_2$  in glass were for a family of soda-silicate glasses [9]. In this case, it was reported that the solubility increased with increasing temperature and with increasing soda content. The solubility at lowest soda content (20%) and at the lowest temperature ( $1000^\circ\text{C}$ ) was about 50 ppm.

Solubility measurements were made using the  $\text{RuO}_2$  powder prepared by drying the hydrate as previously described [10], and pure lead borosilicate glass that was finely ground in the agate ball mill before weighing. Ten weight percent mixtures ( $\text{RuO}_2/\text{glass}$ ) of dried powder were dispersed thoroughly in the agate ball mill, and then heated in platinum crucibles. Samples were heated for 15 minutes to approximate a typical tunnel kiln firing, and for 13 hours to obtain the equilibrium solubility. The firing temperatures used for both time intervals were  $600^\circ\text{C}$ ,  $700^\circ\text{C}$ ,  $800^\circ\text{C}$ ,  $900^\circ\text{C}$ , and  $1000^\circ\text{C}$ . This temperature range was chosen to include the maximum temperatures of kiln profiles.

At the end of the heating period the platinum crucibles were quenched in cold water, in order to minimize the possibility of any reprecipitation of  $\text{RuO}_2$ . The quenched samples were treated for 24 hours with a solution of 30 ml  $\text{HCl}$  + 25 ml  $\text{HF}$  + 20 ml  $\text{H}_2\text{O}$ . Ruthenium dioxide is not dissolved by either of these acids but the ruthenium dissolved in the glass does go into solution along with the glass. The resulting solution was filtered twice to remove the residue and the filtrate was heated at  $100^\circ\text{C}$  until its volume decreased to about 10 ml. It was filtered again to remove the residue and

the filtrate was then analyzed for ruthenium. The residue was also treated with HCl and analyzed for ruthenium. A blank solution was prepared by treating the  $\text{RuO}_2$  powder with HF and HCl in a manner identical with that used for the composite.

The amount of ruthenium in the above solutions was determined using a Perkin Elmer Model 303 Atomic Absorption Spectrophotometer after calibration with a ruthenium solution standard supplied by Spex Industries, Inc. No detectable amount of ruthenium was found in the blank solution, verifying an insignificant solubility of  $\text{RuO}_2$  in HF and HCl, or in the solutions prepared by subsequent treatment of the precipitate.

The results of the test samples are given in Fig. 1. As can be seen, the average concentration of  $\text{RuO}_2$  in glass for typical tunnel kiln firings is about 4 ppm and even at  $1000^\circ\text{C}$  the solubility is less than 50 ppm, consistent with the earlier work of Mukerji and Biswas for soda-silica glasses [9]. For fixed times, the solubility increases with increasing temperature as expected.

The differences between the 15 minute and 13 hour curves of Fig. 1 can be explained in terms of particle size effects. The solution concentration measured with this technique averages the concentration for the glass in the sample both near and far, on a microscopic scale, from the particles of  $\text{RuO}_2$ . For example, it is unlikely that the concentration of  $\text{RuO}_2$  in the glass is uniform after the 15 minute firing. The activity of the  $\text{RuO}_2$  at the surface of small particles is enhanced by the small radius. This increases the concentration of solute at temperature  $T$  by an amount given by

$$\ln \frac{C}{C_0} = \frac{V_o \gamma_{SL}}{RTr}$$

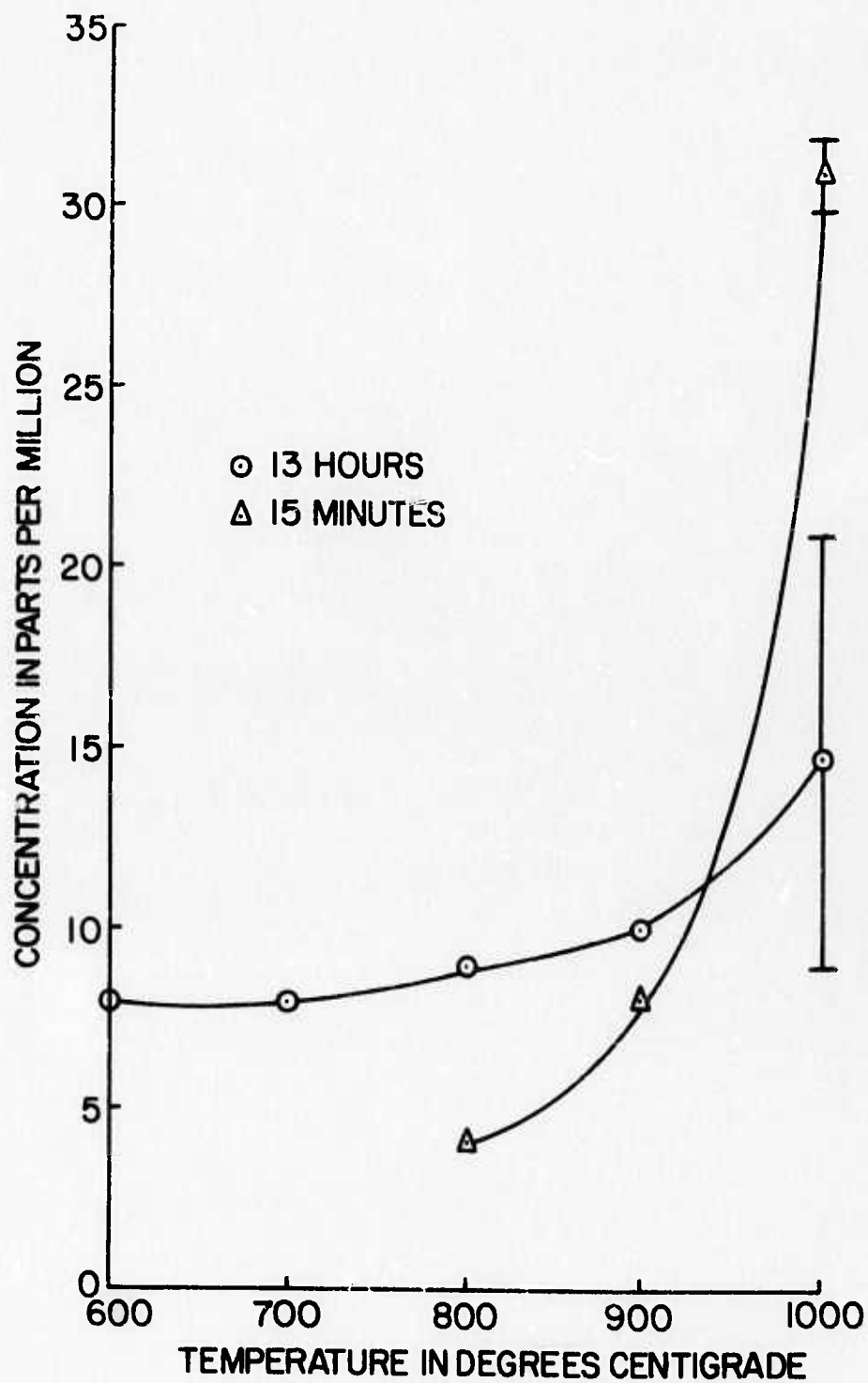


Figure 1. Solubility of Ru in 63% PbO-25% B<sub>2</sub>O<sub>3</sub>-12% SiO<sub>2</sub> Glass

where  $c$  is the concentration at the surface of the particle of radius  $r$ ,  $c_0$  is the concentration at a flat surface,  $V_0$  is the molar volume, and  $\gamma_{SL}$  is the solid-liquid interfacial energy. These effects due to small particle size would explain why the concentration of  $\text{RuO}_2$  in the glass at  $1000^\circ\text{C}$  is greater after 15 minutes than after 13 hours. During initial heating the smallest particles dissolve rapidly, creating a super-saturated solution at the location of the small particles. Then the  $\text{RuO}_2$  diffuses through the glass and precipitates on the surface of larger particles, eventually decreasing the total amount of  $\text{RuO}_2$  dissolved in the glass to the equilibrium value. This reduction in total surface area by the growth of larger particles and annihilation of smaller particles is called Ostwald ripening, and is a destructive force in the development of a conductive network. Therefore, although the concentrations measured in this experiment were low, it is still possible that the concentration of  $\text{RuO}_2$  is large at the particle glass interface.

The  $\text{RuO}_2$  concentration measurements at  $1000^\circ\text{C}$  were repeated, starting with a new  $\text{RuO}_2$ -glass composite to verify the inverted concentrations. The data points at  $1000^\circ\text{C}$  on Fig. 1 are the average of the two values obtained and the error symbols show the discrepancy. The larger error is at the lower concentration, as expected.

#### B. Glass Sintering

Preliminary experiments to demonstrate the sintering of glass particles have been conducted as a prelude to quantitative measurements to be performed at constant temperature or constant heating rate. One of these two temperature conditions is necessary in order to relate sintering rates to material parameters. The conclusion that can be drawn from these

preliminary observations is that it should be possible to obtain a quantitative description of glass sintering.

Figure 2 shows the successive stages during sintering of glass particles of approximately 300  $\mu\text{m}$  diameter. The time and thermocouple emf are recorded on the left side of the screen with a second camera and special effects unit as described earlier [7]. This method of recording data is useful because it creates a virtually continuous and complete record of the sintering process, and all the required data can be taken on the same set of samples. The video monitor also offers the additional advantage of observing rapid processes at high temperatures. This is demonstrated by the four photographs of Fig. 2, for which the total elapsed time is only 30 seconds and yet the number of sequential viewing frames is sufficient for quantitative rate measurements. The data obtained from particles in this size range can be scaled down to obtain rate information for the particle size used in resistor formulations once the dominant sintering mechanism is identified.

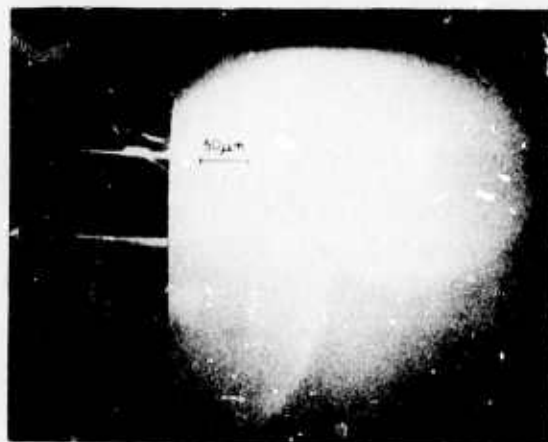
### C. $\text{RuO}_2$ Sintering in Glass

Preliminary experiments to observe  $\text{RuO}_2$  sintering in the presence of glass were conducted utilizing  $\text{RuO}_2$  particles of approximately 100  $\mu\text{m}$  diameter. The  $\text{RuO}_2$ -glass mixture dispersed in a screening agent was applied to American Lava AlSiMag 614 (96%  $\text{Al}_2\text{O}_3$ ) substrates 0.015 inches thick, dried at 300°C for 20 minutes and subsequently fired on the hot stage. Since the glass is optically transparent the  $\text{RuO}_2$  particles can be easily observed in transmitted light after the glass flows.

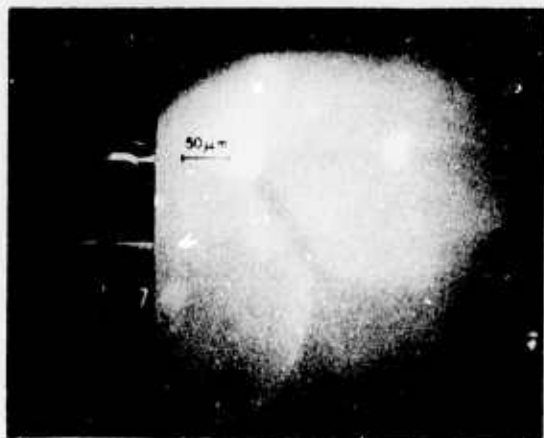
Reproduced from  
best available copy.



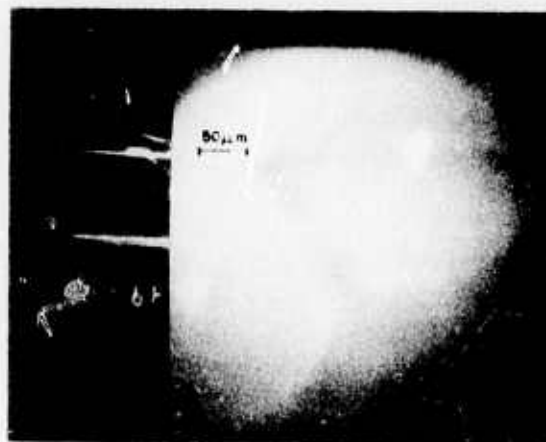
a.



b.



c.



d.

Figure 2. Successive Stages of Neck Growth  
During Sintering of Glass Spheres

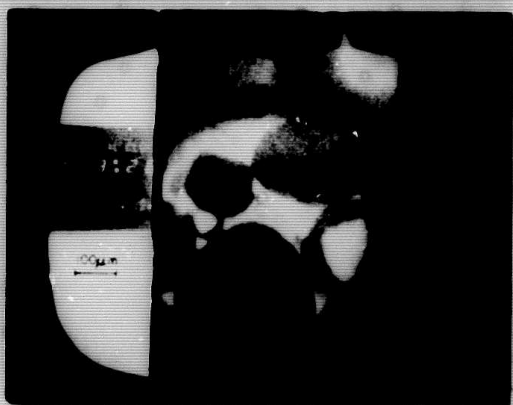


Attempts to observe neck growth between  $\text{RuO}_2$  particles in the presence of glass have not as yet been successful, probably due to the slower rate of sintering at these larger particle sizes, as predicted by the rate equations. It may be necessary to use considerably smaller particles sizes in order to obtain quantitative sintering rates. If the ultimate particle size required is 1  $\mu\text{m}$  or less it will not be possible to use the hot stage microscopy technique. Instead, quenching experiments will be performed and the samples examined using either Scanning Electron Microscopy or Transmission Electron Microscopy.

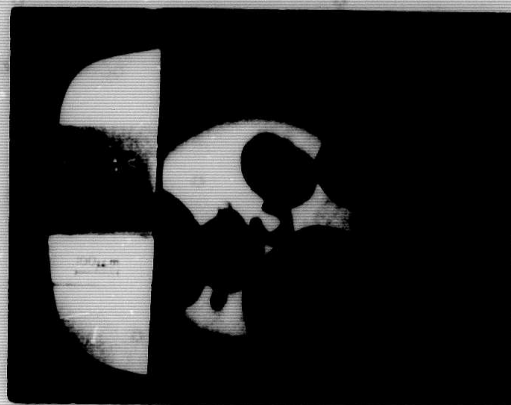
Although sintering was not observed in these samples in reasonable durations of time, gas bubbles and their ability to move the large ( $\sim 100\mu\text{m}$ )  $\text{RuO}_2$  particles were observed. Figure 3, a sequence in the firing of the  $\text{RuO}_2$ -glass composite, shows the movement, toward the surface of the film and to the right of the viewing area of one gas bubble and the resulting motion of neighboring  $\text{RuO}_2$  particles. The bubble was later observed to break at the surface. Figure 4 shows a before-and-after result of bubble movement on the relative position of two  $\text{RuO}_2$  particles. The ability to move these larger particles of  $\text{RuO}_2$  clearly indicates that the gas bubbles can cause the movement of the smaller  $\text{RuO}_2$  particles in resistors and thereby profoundly affect the creation and/or initial destruction of the conductive network. The origin of the bubbles is not known; they could be due to the escape of residual screening agents, a reaction between  $\text{RuO}_2$  and glass, oxidation of  $\text{RuO}_2$  to gaseous  $\text{RuO}_3$  or  $\text{RuO}_4$ , or air entrapment in the glass. The latter seems most likely. Some bubbles still exist at  $800^\circ\text{C}$ .

#### D. Resistor Firing

The firing of resistors has been observed with the hostage video



a.



b.



c.

Figure 3.  $\text{RuO}_2$  Particles in Glass

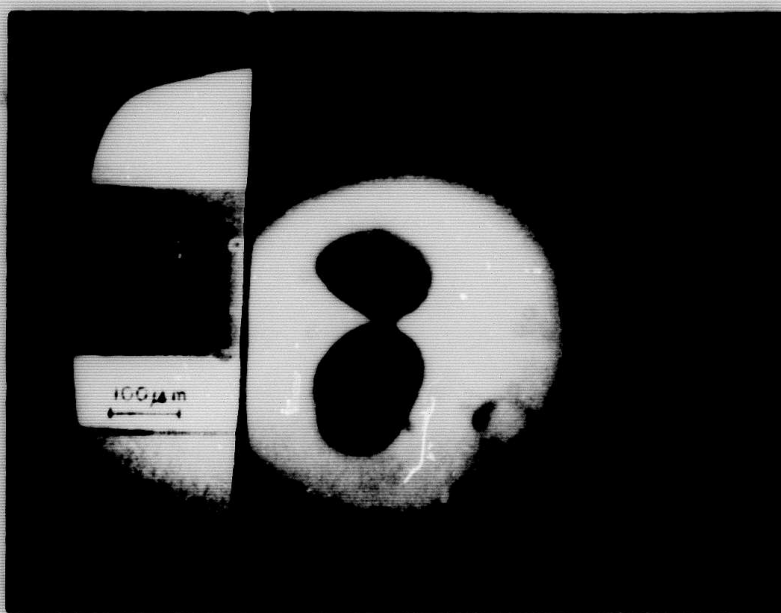
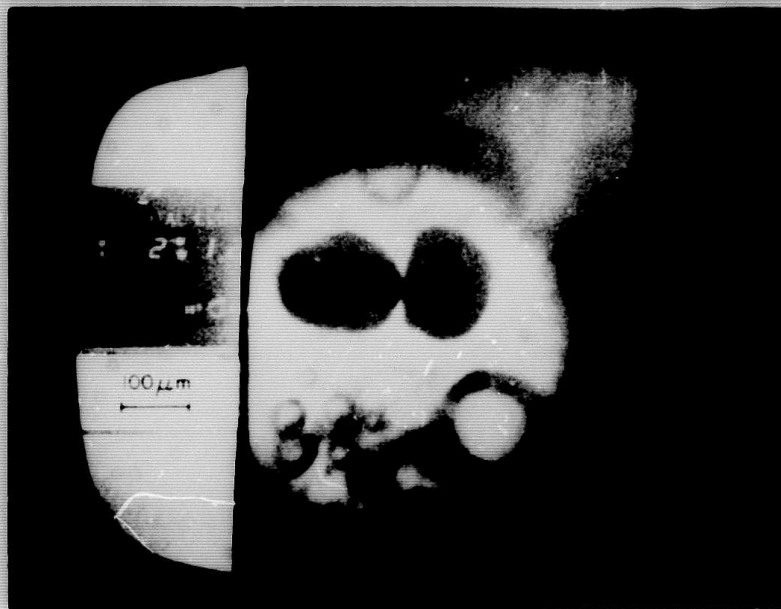


Figure 4. Movement of RuO<sub>4</sub> Particles in Glass



metallograph. No quantitative data have been obtained nor has any reaction been observed that was not anticipated from previous observations with optical microscopy. However, the turbulent nature of the resistor during firing is dramatically shown on the video tape records. After the glass has fused ( $\sim 600^{\circ}\text{C}$ ), the resistor surface, as seen in reflected light, has the appearance of a Yellowstone mudpot. Escaping gas bubbles cause the surface to heave up tens of microns for times the order of one second. The bubble density at  $700^{\circ}\text{C}$  can be estimated from Fig. 5 which shows the surface of a resistor that had been heated slowly for about 1 hour. As the temperature is increased (and the glass viscosity decreases) the bubbles are released with less surface upheaval, but the bubbles are still observed up to  $800^{\circ}\text{C}$ . In fact, the release of bubbles was observed for 60 minutes at a constant temperature of  $800^{\circ}\text{C}$ .

Figure 6 shows the sequential development of a resistor being heated at about  $10^{\circ}\text{C}/\text{minute}$ , viewed with transmitted light to show the  $\text{RuO}_2$ . Experience has shown that the bubbles are almost impossible to see under these conditions and future plans call for alternating the type of light during firing to better relate the existence of moving bubbles to the dispersion of the  $\text{RuO}_2$  powder. However, during the time that the bubbling actions exists, the  $\text{RuO}_2$  becomes more agglomerated, resulting in increasing areas of white in the photomicrographs. Optical photomicrographs of quenched samples showing similar results are discussed later.

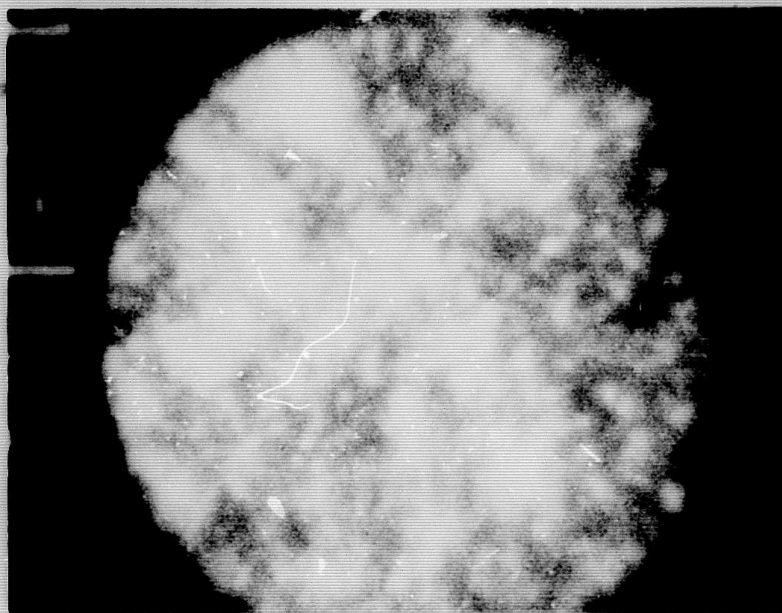
The conclusion that can be drawn from these observations is that the resistor film is in a dynamic state of agitation throughout the firing process. This fact is very important for any model describing microstructure development.

Reproduced from  
best available copy.

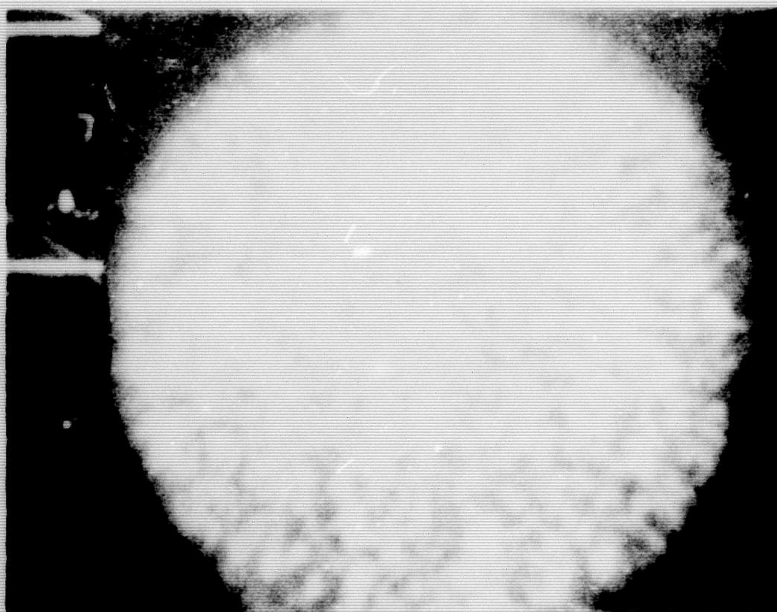


Figure 5. Resistor Surface at 700°C Showing Gas Bubble Density





a. 550°C



b. 800°C

Figure 6. Resistor Network Development

### E. New Phases

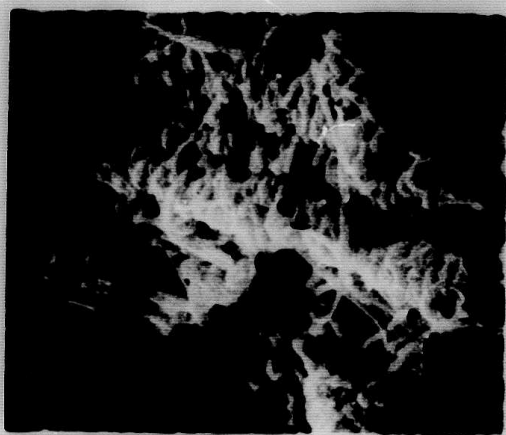
Though the possibility of new phase development (regions other than glass and particulate  $\text{RuO}_2$  such as semiconducting glass) has been proposed, earlier electrical measurements have failed to detect any new electrically active phases [8]. SEM investigation has, in isolated cases such as very long firing times, revealed a variety of shapes that are neither vitreous lead borosilicate glass nor  $\text{RuO}_2$  particles. Some of these are shown in Fig. 7. The small size of the configurations causes a problem in using the SEM X-ray analyzer to identify the composition of a specific region in the resistor. The penetration depth of the electron beam is greater than the dimensions of the new phases shown in the figure and so elements below the new phase are detected also. For example, analyses of the crystals of Fig. 7d typically indicate the presence of ruthenium and aluminum. (Significant amounts of aluminum are to be expected in a fired resistor because of the substrate.)

As an additional investigation of new crystalline phases a series of experiments were performed by X-ray diffraction using a Phillips Norelco Diffractometer. Samples were prepared in the following ways:

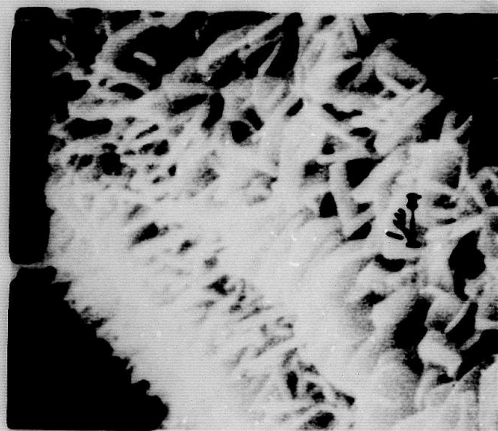
1. The paste containing 10 w/o  $\text{RuO}_2$  was hand printed on alumina substrates (2" x 1"), dried at  $300^\circ\text{C}$  for 20 minutes, and fired at  $800^\circ\text{C}$  for different times, ranging from 15 minutes to 40 hours. Blank samples were prepared from glass fired on alumina substrates using the same heat treatments as those of the resistors in order to eliminate the extra phases due to the substrate material and possibly the glass.

2. The paste containing 10 w/o  $\text{RuO}_2$  was screen printed on alumina substrates, dried at  $300^\circ\text{C}$ , and then heated at  $500^\circ\text{C}$  for 30 minutes,  $625^\circ\text{C}$  for 30 minutes, and  $800^\circ\text{C}$  for 15 minutes. The samples heated at  $800^\circ\text{C}$  were

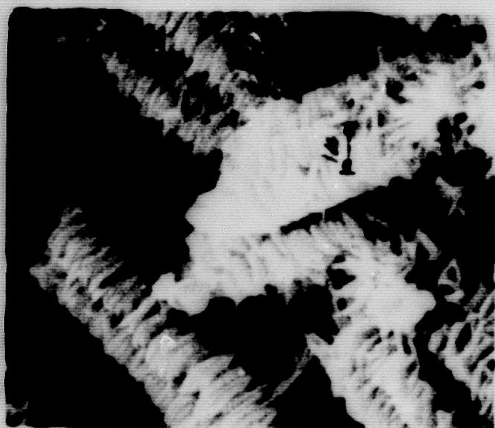




a.



b.



c.



d.

Figure 7. Crystalline Structures Formed During Resistor Firing



:8

treated with HCl until all resistor material was removed from the substrates. The resulting solution was placed on glass slides and dried to form a powder residue for the X-ray diffraction. Similar blank samples were prepared by using the identical process with a glass paste containing no  $\text{RuO}_2$  in order to check for any phases formed in the glass or as a result of chemical action between the glass and HCl.

Some of the same samples, fired at  $500^\circ\text{C}$ ,  $625^\circ\text{C}$ , and  $800^\circ\text{C}$ , were treated with HCl and filtered to collect the residue which was then washed with hot water to dissolve the  $\text{PbCl}_2$ . The remainder of the samples were treated with both HCl and HF, to remove  $\text{SiO}_2$  as well as PbO. This was done with the following sequence: Treat with HCl to form  $\text{PbCl}_2$  and rinse with hot water to remove the  $\text{PbCl}_2$ . Treat the residue with HF and remove the  $\text{SiF}_4$  by filtering. Rinse with hot water to remove the  $\text{B}_2\text{O}_3$ .

3. The paste containing 10 w/o  $\text{RuO}_2$  was placed in a platinum boat, dried at  $300^\circ\text{C}$  for 20 minutes, and heated at  $800^\circ\text{C}$  for times ranging from 15 minutes to 20 hours. The fired samples were treated with HCl, HF, and hot water as described in 2. above.

4. In a previous report [11] the preparation of the massive  $\text{RuO}_2$ -glass composites used for the electrical resistance measurements was described; they had been heated at  $900^\circ\text{C}$  for 16 minutes. They were ground into a powder for direct analysis.

Several observations were made during these four series of experiments:

1. The X-ray diffraction measurements of the four types of samples described above failed to indicate the formation of any new crystalline phase, and hence, it can be concluded that either no new crystalline phase formed or that the new phases formed are in a quantity or size that is below the detection limit of the X-ray diffractometer.

2. The resistor paste that was heated in the platinum boat contained metallic ruthenium in early stages of heating that was then slowly oxidized during the remainder of the firing period. The ruthenium metal is believed to be formed through reduction of the  $\text{RuO}_2$  by the decomposition products of the screening agent. Rapid reduction of  $\text{RuO}_2$  and slow oxidation of ruthenium is consistent with earlier observations. Because of the large surface area to volume ratio in the screen printed samples, most of the organic material is removed during initial drying and hence no ruthenium metal was detected in any screen printed sample. However, this is an example of the importance of the atmosphere during firing of thick film resistors.

3. It was observed that the  $\text{RuO}_2$  peaks from the diffractometer for the samples fired at  $800^\circ\text{C}$  became narrower with longer firing times. The sharper peaks could be due to: (1) an increase in average particle size caused by growth of larger particles at the expense of small particles or the dissolution or evaporation of small particles; (2) grain growth within each particle; or (3) a decrease in internal strain of the particle, such as by a reduction in the concentration of crystal defects. The dominant mechanism has not been determined. However, it has been determined that the  $\text{RuO}_2$  powder used to make the resistors undergoes the same line narrowing when heated at  $800^\circ\text{C}$  in the absence of glass, as does the powder in the resistors.

Although the experiments described above failed to detect new phases, Fig. 7 shows that new phases do form on certain occasions. In particular, the crystals shown in Fig. 7d have been observed frequently. These crystals have been detected by X-ray analysis and they have also been detected in glass-on-alumina samples that contained no  $\text{RuO}_2$ . Thus, although the crystals have not been identified from their X-ray pattern, it is known that ruthenium is not part of the crystal structure.

### III. Resistor Firing

Earlier experiments monitoring the resistance of resistors during firing have shown that they all follow the same basic development sequence. In particular, sample 35, [12] fired at  $590^{\circ}\text{C}$  for 550 hours, decreased in room temperature resistance in the early portions of its life to a minimum at 50 hours and then increased in resistance until at least 350 hours, while the TCR remained negative. Somewhere in the interval between 350 hours and 420 hours the electrical properties changed significantly; the TCR became positive ( $+200\text{ppm}/^{\circ}\text{C}$ ) and the room temperature resistance decreased. In the early portions of the firing ( $< 350$  hours) the resistance at  $590^{\circ}\text{C}$  was independent of the room temperature resistance; whereas, at the end of the firing the high and low temperature resistances were similar. These results were shown to be consistent with the proposed conduction model. Additional experiments using the same resistor paste and a new resistor paste have been performed. These samples were similar in electrical properties, as described below.

#### A. Old Paste

Although sample 35, fired at  $590^{\circ}\text{C}$  for 550 hours, yielded valuable insight into the development of the conductive network, the slow rate of formation resulted in excessive experimental time. Thus, an increased temperature ( $640^{\circ}\text{C}$ ) was selected in order to achieve more rapid network development, but still maintain network development times long compared to the time required to quench the samples to obtain room temperature resistance measurements at periodic intervals during the firing.

Figure 8 shows the resistance versus time of several samples fired at  $640^{\circ}\text{C}$ . The same basic behavior is observed for all samples: the

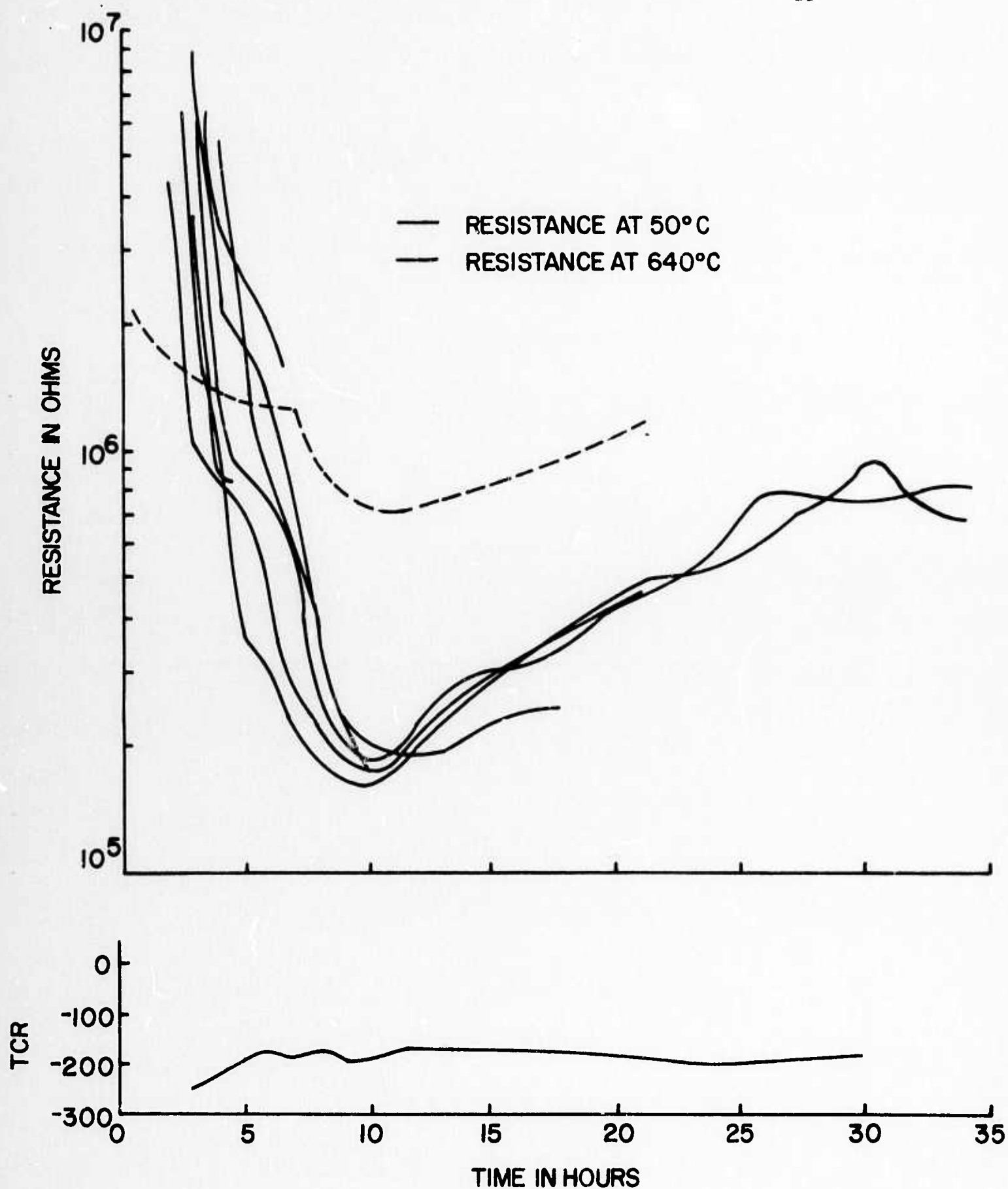
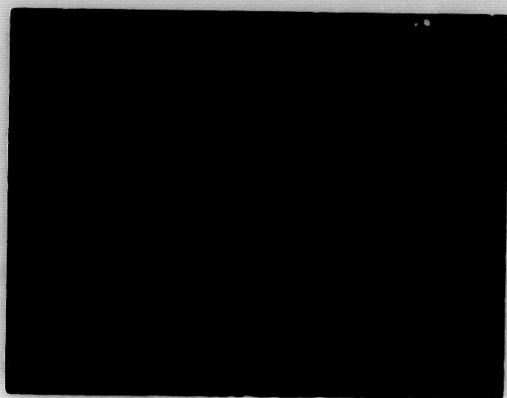


Figure 8. Resistance and TCR versus Firing Time for 640°C  
Maximum Temperature

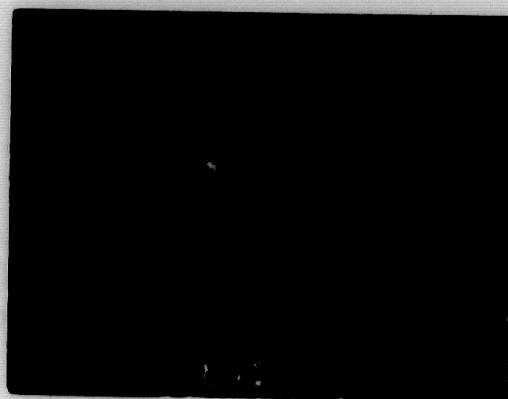
resistance decreases from an initial infinity to a minimum at approximately 10 hours and then increases monotonically. The TCR increases early in the life of the sample but remains negative throughout the firing period. This negative TCR behavior is typical of this paste; the positive TCR observed after 350 hours in the 590°C firing was the only example of a positive TCR in about 25 samples. Part of the resistance increase at times greater than 10 hours is due to a high resistance interface at the platinum conductive [13] and the TCR and resistance data are not valid representations of the resistor for times in excess of 20-25 hours.

The samples represented in Fig. 8 were prepared to demonstrate that the room temperature resistance versus firing time is repeatable for identical samples and firing profiles and, therefore, that samples can be prepared in definable stages of development. The seven samples were terminated at firing times of 2-1/2, 4-1/2, 6-1/2, 10, 21, and 72 (2 samples) hours in order to directly analyze the developing microstructure. It can be seen from the graph that the resistance spread in sample resistance minimizes at the minimum in resistance value and that the resistances do not diverge greatly from that point on. However, the resistance spread before the resistance minimum is much greater; in some cases they differ by a factor of ten. The sequential optical photomicrographs of Fig. 9 show the same development shown earlier in Fig. 6. The increasingly larger white areas (transmitted light) show a decrease in the uniformity of  $\text{RuO}_2$  dispersion. The magnification of the photomicrographs is only 40X, and the microstructure predicted by the proposed microstructure model cannot be seen at this magnification. However, beyond 10 hours, the increasing open areas that are void of  $\text{RuO}_2$  do represent, on a macroscopic scale, a destruction of the conductive network.

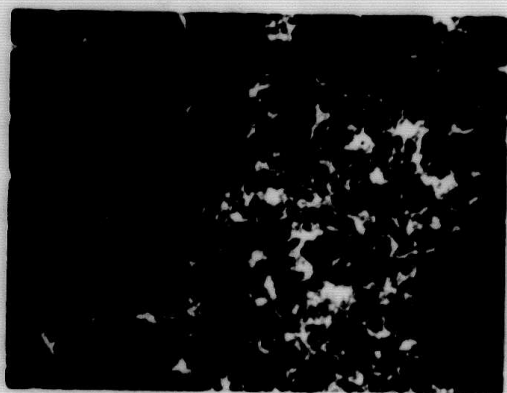




a. 4.5 hours



b. 6.5 hours



c. 10 hours



d. 21 hours

Figure 9. Resistor Macrostructure Development at  $640^{\circ}\text{C}$  (40X)

Several other resistor samples have been fired at temperatures from  $600^{\circ}\text{C}$  to  $650^{\circ}\text{C}$  and quenched frequently to determine room temperature resistance and TCR. Graphs of the results always appear similar to Fig. 8 and that of sample 35 ( $< 350$  hours); only the time axis (rate of development) changes.

The necessity for proper storage of resistor pastes was definitely demonstrated by this particular formulation. Storing the jar of paste at rest or on slow roller storage for periods of approximately one month caused the  $\text{RuO}_2$  to agglomerate in the paste, sometimes enough to be seen in the fired resistor with the naked eye. A few minutes of roller milling was sufficient to redisperse the powders and this sometimes decreased the resistance by as much as 30%.

#### B. New Paste

Because of the moderate volume in anticipated industrial coupling experiments and a desire to be able to correlate results from different types of scientific experiments, several hundred grams of 5%  $\text{RuO}_2$  and 40%  $\text{RuO}_2$  end member pastes were prepared as described later. A 10%  $\text{RuO}_2$  blend was then prepared for all future individual firing experiments. It was immediately noted that this newer paste, though containing virtually the identical  $\text{RuO}_2$  content, had a different rate of conductive network formation and different resistance value, although the shape of the graph remained basically the same. As a result of the observed differences, several comparative investigations were begun; these are discussed in later sections, except for the resistance and TCR as a function of temperature and time, reported here.

Figures 10 and 11 represent typical characteristics of the new paste. Fig. 10 shows the resistance at both  $610^{\circ}\text{C}$  and room temperature; they both decrease from an initial infinity to a minimum at 8 hours and then increase slowly. Figure 8 showed that the old paste required a firing temperature of  $640^{\circ}\text{C}$  to reach a minimum at 8 hours and the minimum resistance was  $200\text{K}\Omega$  as compared to  $3\text{K}\Omega$  for the sample of Fig. 10. It can also be seen that the resistance versus time at  $610^{\circ}\text{C}$  was close to the value at room temperature throughout the entire firing period, especially after the first few hours.

The TCR, shown on Fig. 11, is originally highly negative, on the order of  $-450$  ppm, and increases rapidly with firing. The TCR crosses zero before the resistance is a minimum and continues positive until it reaches about  $+125$  ppm at 10 hours, after which it is approximately constant. This more rapid network formation and early, positive TCR becoming constant at about  $150$  ppm/ $^{\circ}\text{C}$  has been common of all samples prepared with the new paste, except one whose TCR continued positive at a nearly linear rate of  $4$  ppm/ $^{\circ}\text{C}/\text{hour}$  until the TCR was  $730$  ppm at 300 hours.

It is common for thick film resistors to have non-linear resistance versus temperature characteristics near room temperature, and resistors made with the new paste are consistent with this rule. Figure 12 shows normalized resistance versus temperature of three samples fired for 20 minutes, 40 minutes, and 90 minutes at  $630^{\circ}\text{C}$ . These figures show the importance of making TCR measurements over the same range of temperatures to make comparisons between samples, at least for the simple resistor system used in this work.

### C. Conduction Mechanisms

The results of these resistor firing studies suggest the existence of two conduction mechanisms that may also coexist in typical tunnel kiln fired



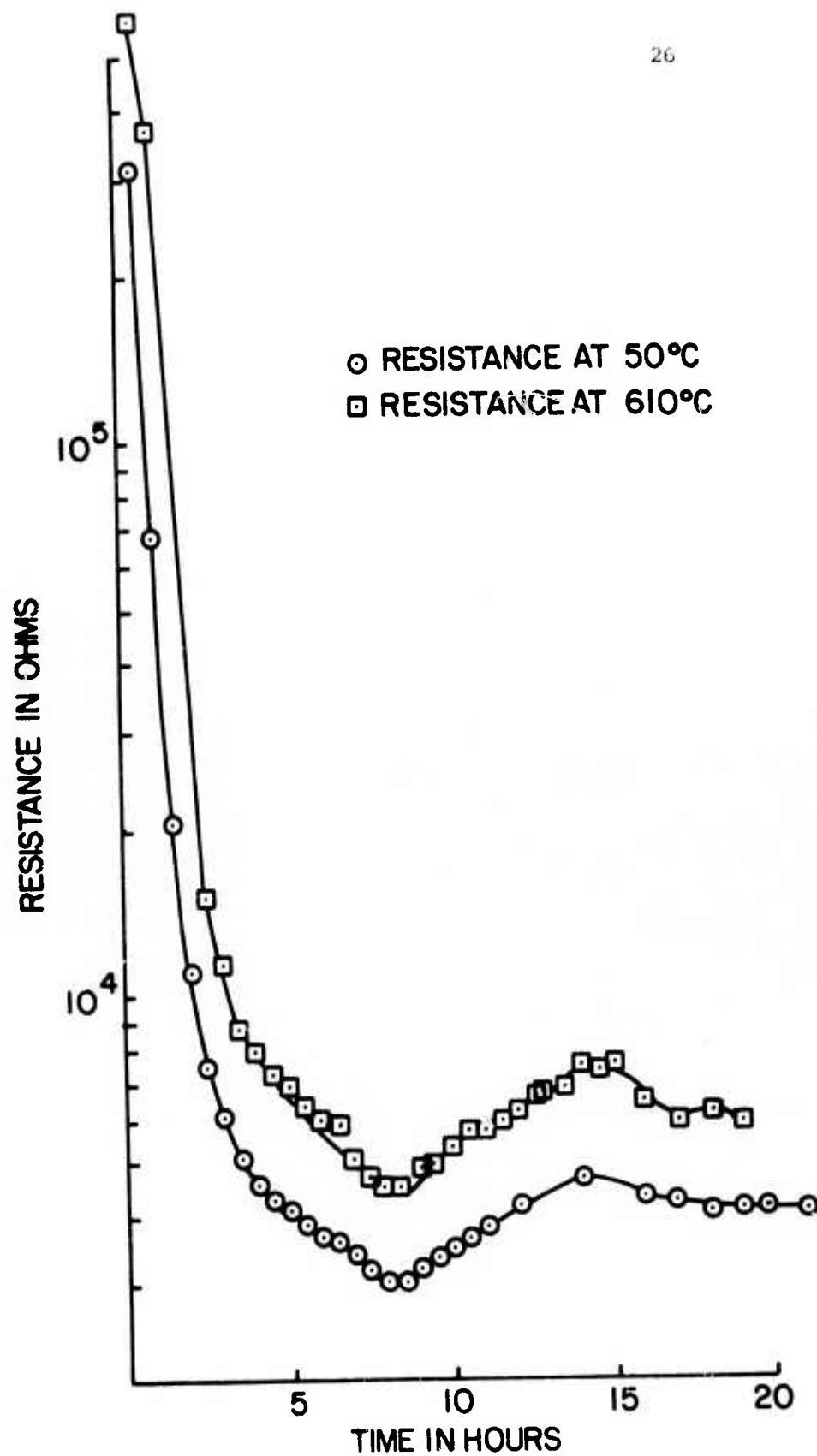


Figure 10. Resistance versus Firing Time for 610°C  
Maximum Temperature

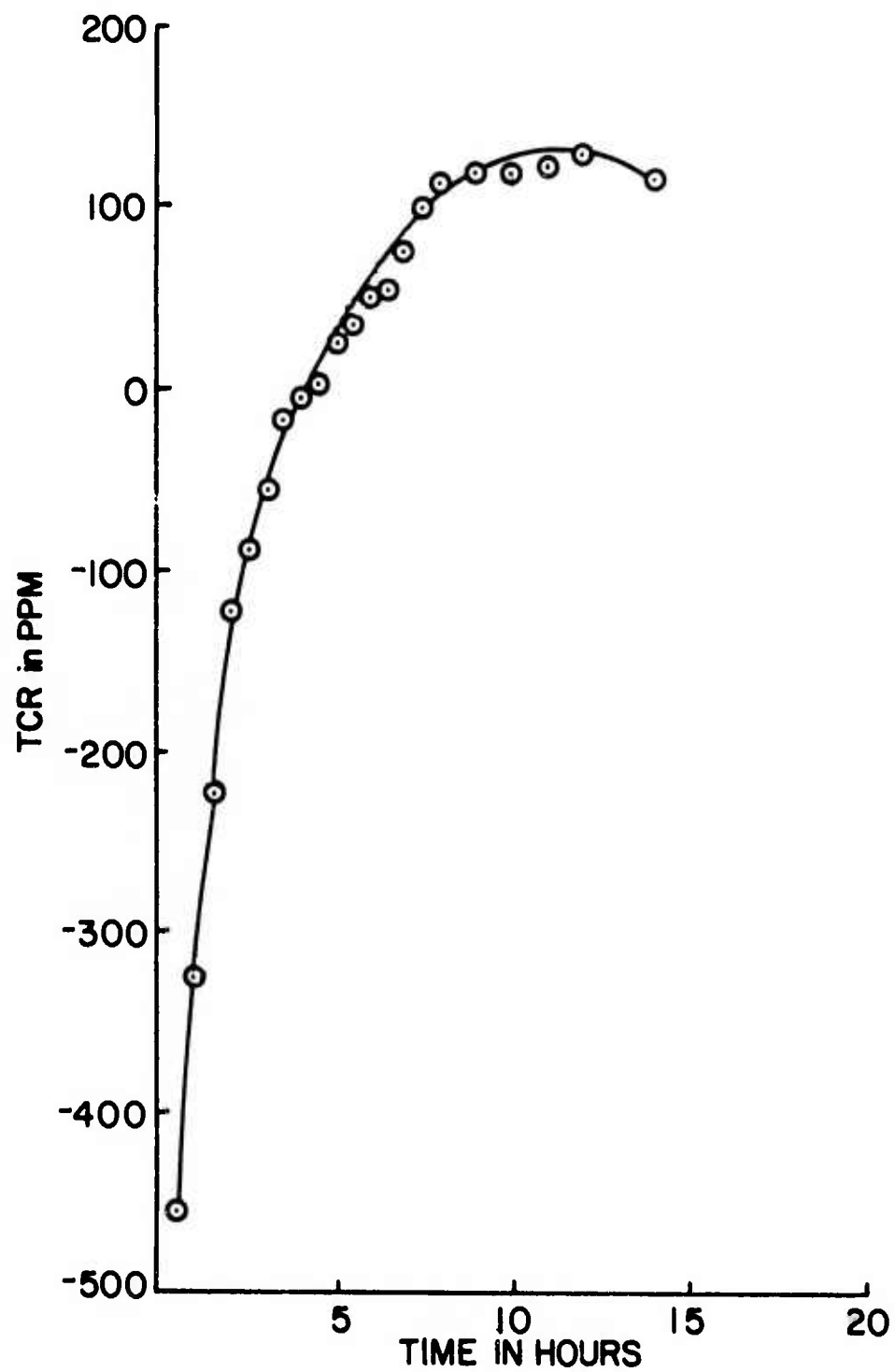


Figure 11. TCR versus Firing Time for 610°C Maximum Temperature

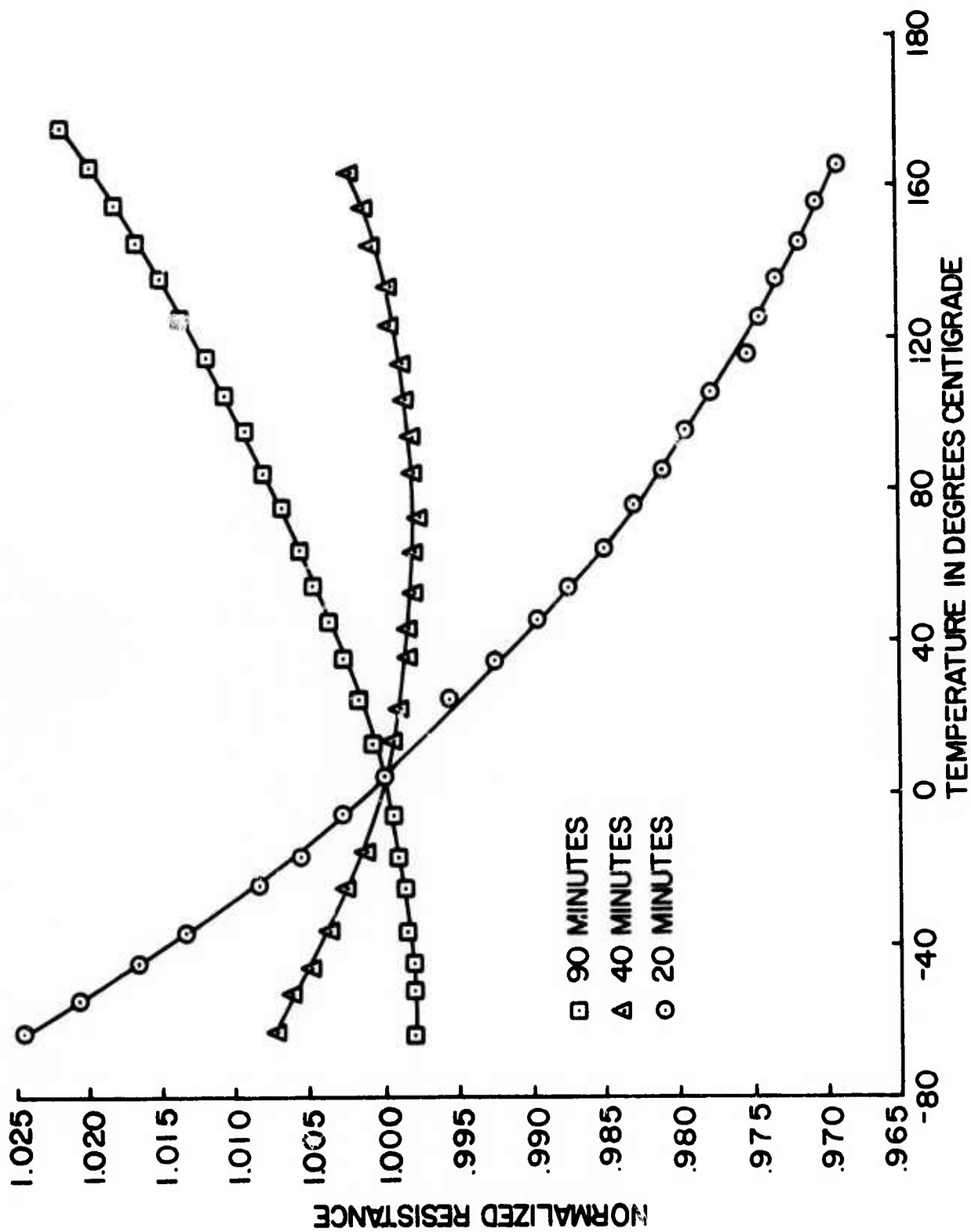


Figure 12. Normalized Resistance for Various Firing Times at 630°C

resistors. One is the result of a sintered  $\text{RuO}_2$  network in the glass matrix as described in the sequential sintering model, and the second involves charge transport on a particle-to-particle basis or through a thin glass film. In the first model, since the  $\text{RuO}_2$  is sintered, the conductive network is independent of the state of the glass and therefore does not change appreciably as the glass is heated through its softening temperature. Because massive single crystal  $\text{RuO}_2$  has a TCR of + 5000 ppm the sintered network might be expected to have a positive TCR, although greatly reduced from that of massive  $\text{RuO}_2$ , due to the increased temperature independent defect scattering in the small particles, and in the sintered neck due to glass impurities. This conductive structure is dominant in Sample 35 for times beyond 400 hours and in the sample represented by Figs. 10 and 11. In both of these cases the resistances at high temperature is only slightly greater than the resistance at room temperature and the TCR is positive, although only + 200 ppm. Though not shown in graphs here, the resistance versus temperature is nearly constant as the glass is heated through the softening temperature as opposed to a bump in the graph as has been observed with some samples [14, 15].

The second possible mechanism involves a conductive network of unsintered or poorly sintered  $\text{RuO}_2$  particles held in direct contact or with a thin film of glass at the interface by rigid glass when cooled and by interfacial forces when the glass is more fluid (near and above the softening temperature). It is difficult to predict the temperature dependence of resistance; the network could have either a positive or negative TCR near room temperature, but some resistance change would be expected near the softening point of the glass. Examples of this network behavior are the first 350 hours of sample 35 and the first 6 hours of the sample represented

by Fig. 8. After 6 hours, Fig. 8 shows a combination of both conduction mechanisms with the unsintered network dominating. Although the high temperature resistance follows the shape of the low temperature resistance, it is 4 times as great and the TCR is negative. Resistor samples whose high temperature resistance is independent of room temperature resistance always show rapidly changing resistance versus temperature as the glass is heated through the softening temperature [15] and frequently, at high temperature there is no electrical evidence of the conductive network that exists at lower temperatures. Because the unsintered network is strongly dependent on interfacial forces, positive TCR's could exist. These have been observed [14].

The two conduction mechanisms can be evoked to explain another observed difference in the electrical properties of the new and old pastes which occurs during the initial firing to high temperature. This is shown in Fig. 13 where the time axis is arbitrarily chosen to be zero at  $513^{\circ}\text{C}$ , and both samples are at the constant temperature of  $625^{\circ}\text{C}$  beyond 8 minutes. The resistance of the old paste decreases slowly during the temperature rise, in a way that is characteristic of glass conduction. However, the new paste decreases three orders of magnitude in several seconds and then increases to approximately the resistance of the glass. This decrease in resistances occurs concurrently with the volume shrinkage of the glass as it sinters and flows, and could be due to particle-to-particle contact of dry  $\text{RuO}_2$  particles caused by the densification of the glass. The subsequent increase in resistance could be caused by the  $\text{RuO}_2$  being wet by the glass and electrically isolated. A conductive network reforms at a later time when the interfacial forces become more dominant and further mixing by gas bubbles helps to pull the particles into closer contact. Fig. 14 shows SEM photomicrographs of dried

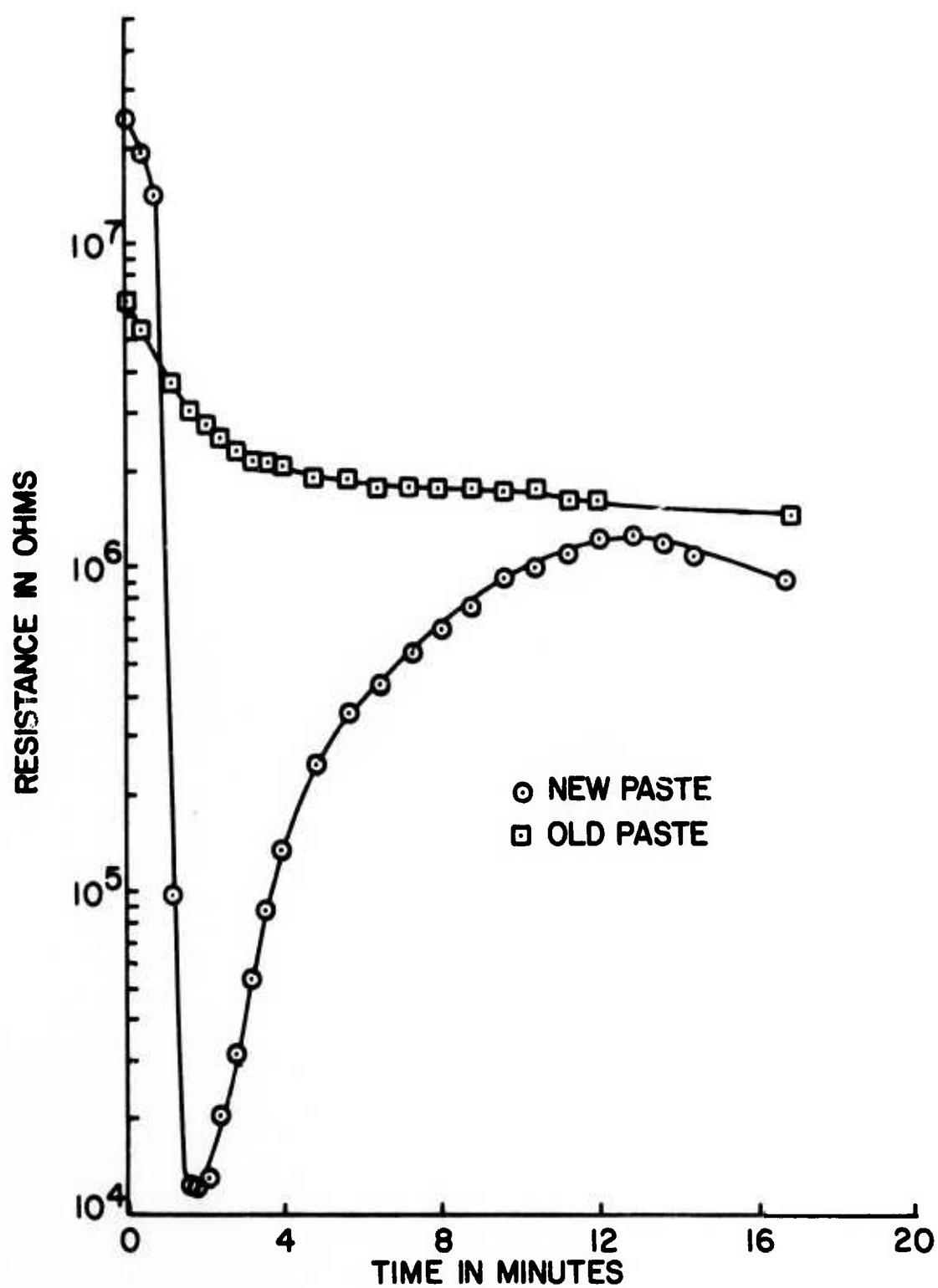
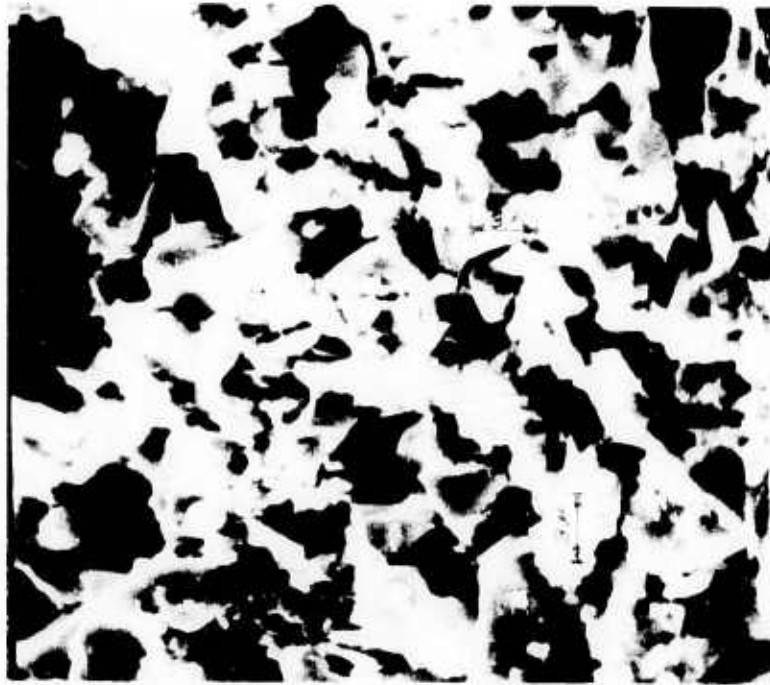


Figure 13. Resistance Changes During Firing From  $513^{\circ}$  to  $625^{\circ}\text{C}$



a. Old Paste



b. New Paste

Figure 14. Dried Resistors Prior to Firing

but unfired resistors made from the two pastes. The large irregular particles are glass, and the clusters of much smaller particles are  $\text{RuO}_2$ . The photomicrographs show a much more uniform dispersion of  $\text{RuO}_2$  in the loose structure of the new paste; the  $\text{RuO}_2$  is less evident in the old paste. Apparently, the less uniform dispersion of the  $\text{RuO}_2$  in the old paste does not permit an electrically continuous structure during densification.



#### IV. Industrial Coupling

The basic goal of this project is to be able to relate materials parameters to resistor and conductor properties so that improved control can be established in industrial fabrication of thick film microcircuits. This requires adequate scientific understanding and previously reported experiments under the present program have been directed toward this goal. However, it is desirable as part of this program to establish a micro-circuit fabrication capability at least similar to typical industrial equipment so as to be better able to make specific, tested recommendations to obtain better predictability, uniformity, and reliability in thick film microcircuits.

The initial plan for coupling with industry was to establish a liaison with one or more companies and thereby use their equipment for preparing printing pastes, drying and firing, etc. This plan was not implemented because of the small scale of the operation required, and because of the reluctance of companies with a long history of secrecy in thick film development to enter into the type of open program that would be required. The alternative was to establish an adequate but limited industrial capability in the laboratory. The equipment required for this has been obtained and consists of the following:

Description	Function
Paddle Blender and Three Roll Dispersion Mill	Prepare printing pastes
Wells-Brookfield Viscometer	Characterize pastes and test uniformity
Aremco Semi-automatic Screening Machine	Screen print pastes onto substrates

Description	Function
Oven	Drying printed pastes
Tunnel Kiln	Fire Resistors & Conductors

The oven is a standard general type of laboratory oven and all other pieces of equipment except the tunnel kiln have been described earlier. They were acquired to provide uniform samples for scientific experiments. The tunnel kiln is the most recent purchase and was necessary to complete the industrial capability. Of course, the kiln and dispersion mill are smaller than typical industrial versions because the laboratory quantities are smaller.

#### A. Tunnel Kiln

The tunnel kiln is shown in Fig. 15 and is schematically represented in Fig. 16. It is a Lindberg laboratory phototype tunnel kiln designed for thick film applications. The basic design incorporates a multiple section heating assembly, a speed-controlled belt, and an atmosphere control system.

The heating assembly has six 6 inch sections controlled by three time proportioning temperature controllers adjustable from 200 to 1200°C. The heater sections can be connected to the controllers in any combination. For the present application the first zone contains one section, the second zone three, and the third zone contains two. Over-temperature protection is provided by a control meter relay driven by a thermocouple that can be installed in any of the six heating elements. The three inch square cross-section fused quartz muffle is used because it is not a source of contamination and is transparent to infra-red radiation. The output end of the kiln contains a 24 inch long water cooled inconel jacket to cool the substrates to room temperature before exiting the kiln. With the kiln profiles currently in use, it is not necessary to use the jacket and so it has been drained.



Figure 15. Lindberg Tunnel Kiln

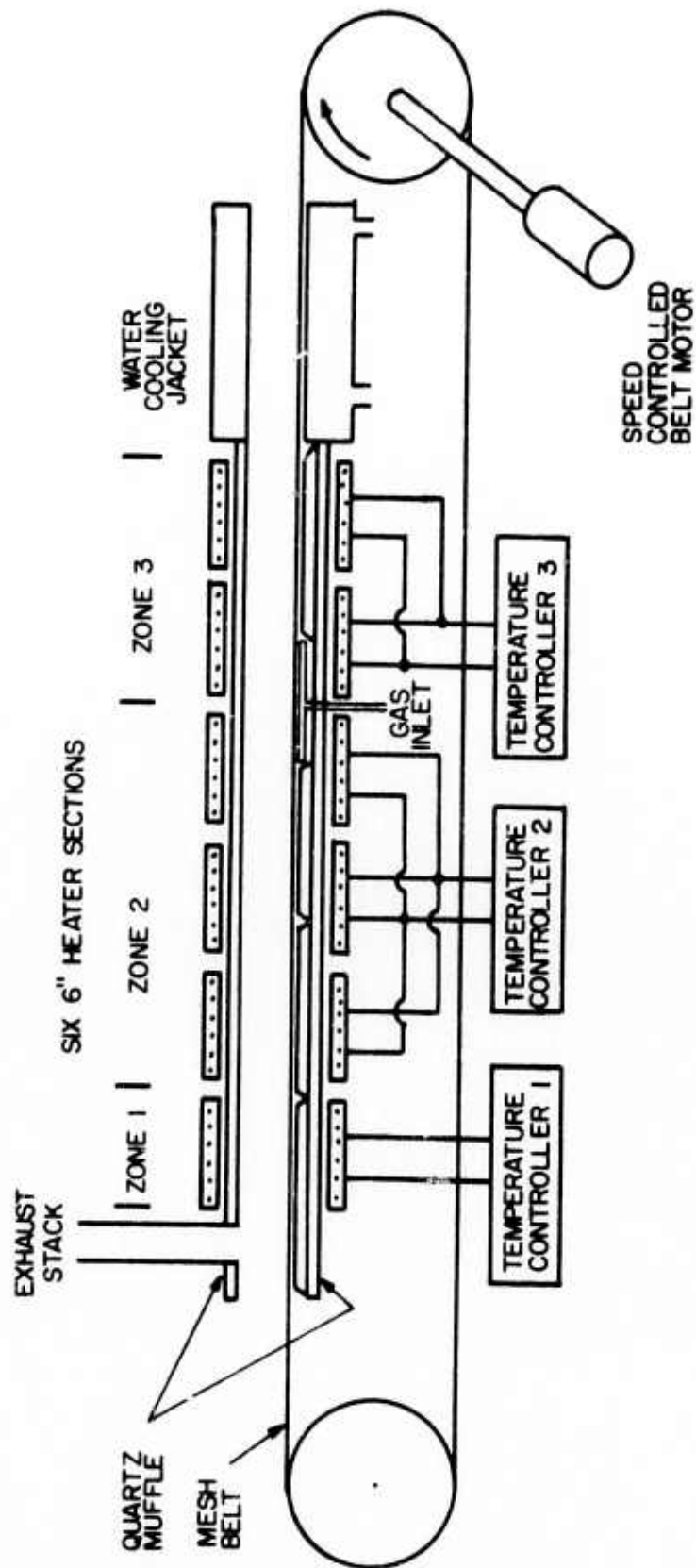


Figure 16. Tunnel Kiln Schematic

Substrates are carried through the kiln on a 2 inch nichrome mesh belt driven by a speed controlled DC motor that can maintain constant belt speeds from 0.3 to 11 inches/sec. Parts are removed by a gravity operated ramp which delivers the parts to a box mounted at the end of the kiln.

The atmosphere can be controlled in the quartz muffle and water cooled jacket by introducing gas beneath the belt between the second and third zones. The atmosphere is contained in the kiln by adjustable openings in the two ends of the kiln and exhausts at the adjustable venting stack. Gas flow rate can be adjusted by a flow meter. No artificial atmosphere is currently used in the kiln because all possible precautions are taken to completely remove screening agents from the resistors before they are placed in the kiln.

The profile initially established in the kiln was chosen to fire 10% RuO<sub>2</sub>/Glass resistors to a minimum in the resistance versus time curve with a belt speed that was in a convenient and dependable range. This was found with zone controller setting of ~~425°C~~ <sup>500°C</sup> and ~~775°C~~ <sup>700°C</sup>, respectively and a belt speed of 4.3 inches/min. Fig. 17 shows the temperature versus distance profile as determined with an 18 gauge Chromel-Alumel thermocouple wired to the belt, a standard technique in the thick film industry. Fig. 18 shows the temperature versus time profile corresponding to the 4.3 inches/minute belt speed. Fig. 19 shows the variation of room temperature resistance versus belt speed, indicating the minimum in resistance value. Previous experiments have determined that resistance value scatter at the minimum is small and, therefore, has the smallest sensitivity to small changes in belt speed. Seventy-two substrates fired in random small samples had an average value of  $984 \pm 3.0 \Omega$ . The profile shown in Fig. 18 will be used to determine the blending curve for the end member pastes, and the effects of firing resistors

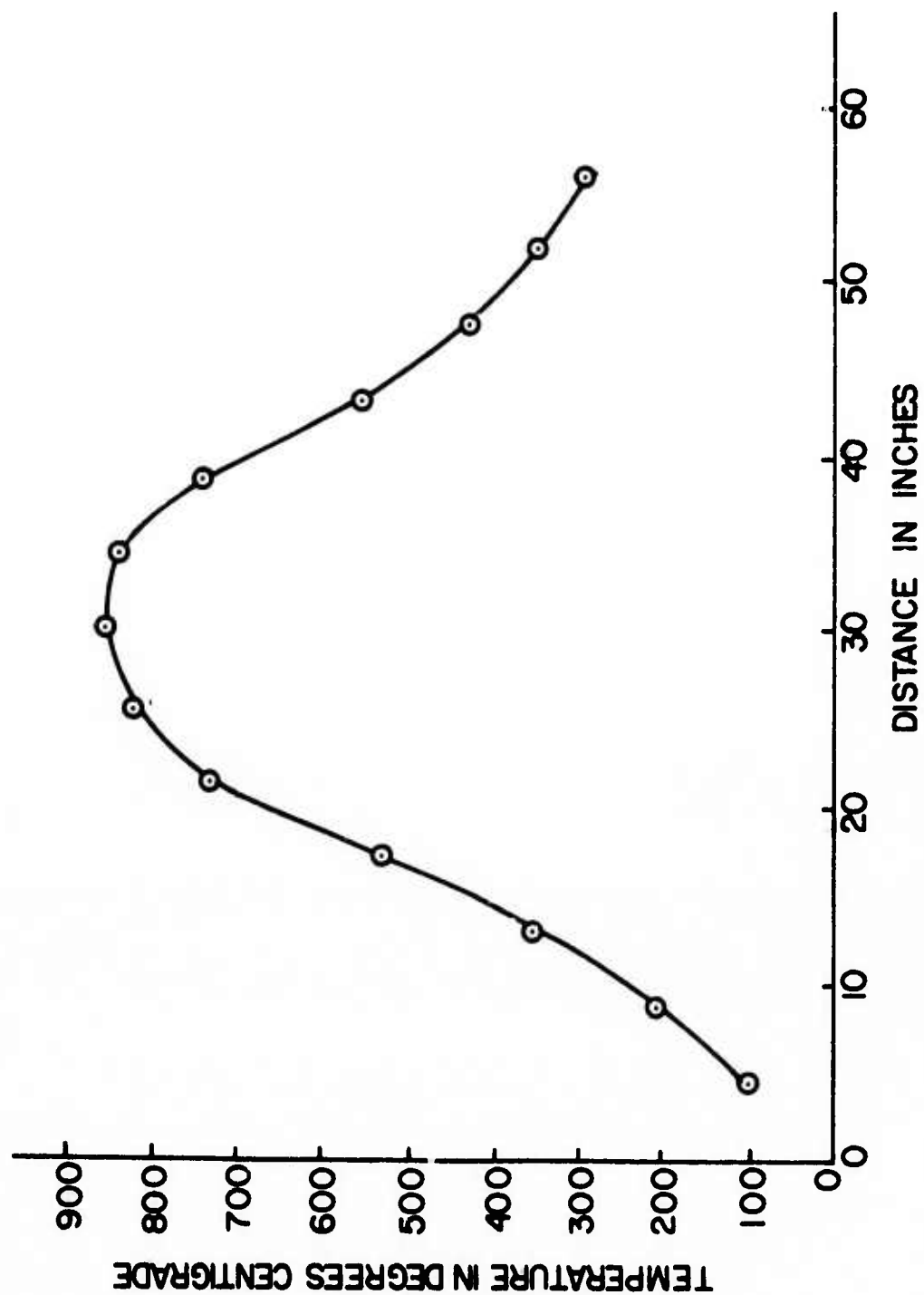


Figure 17. Turnel Kiln Temperature Gradient



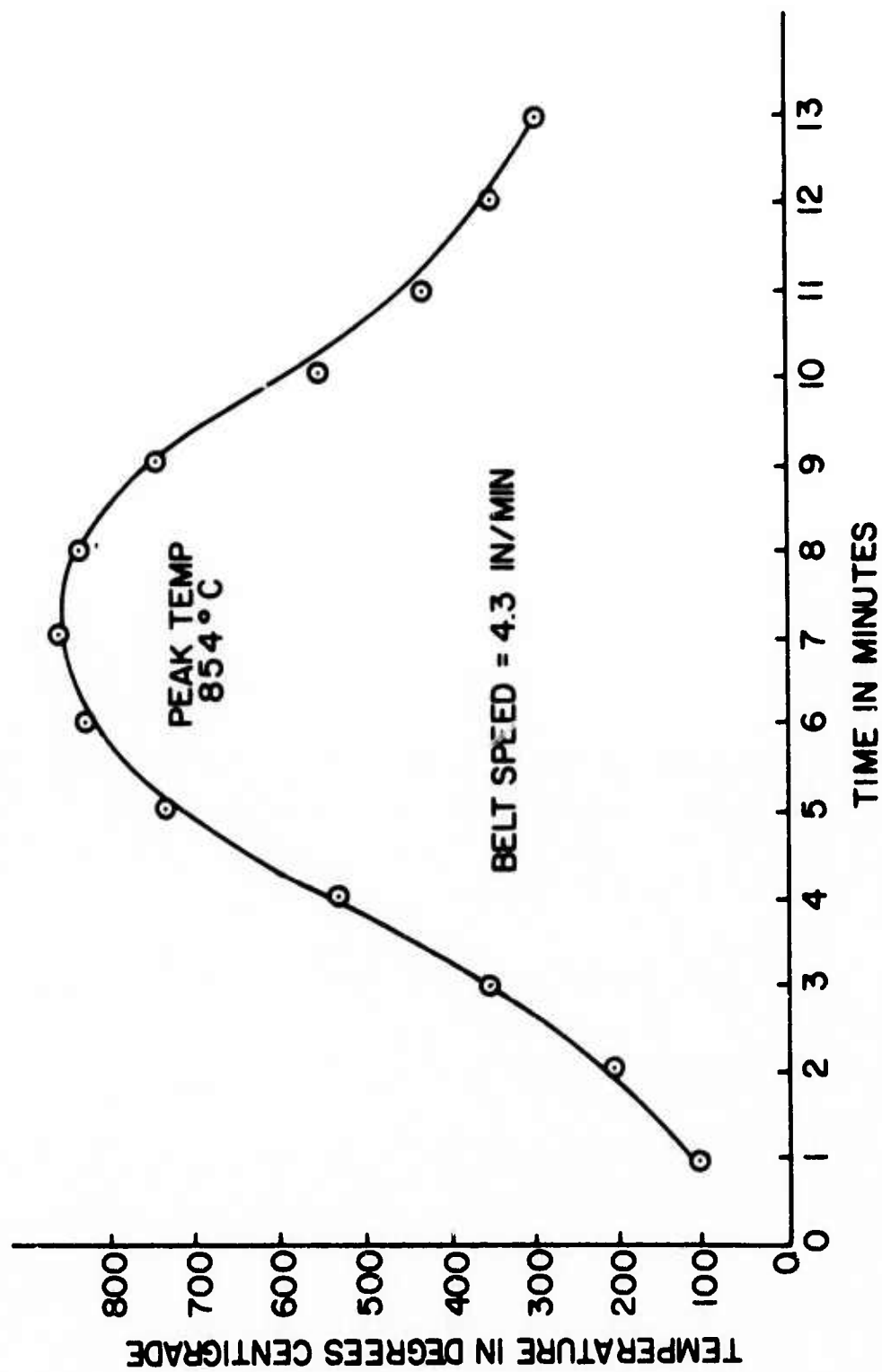


Figure 18. Standard Time-Temperature Profile

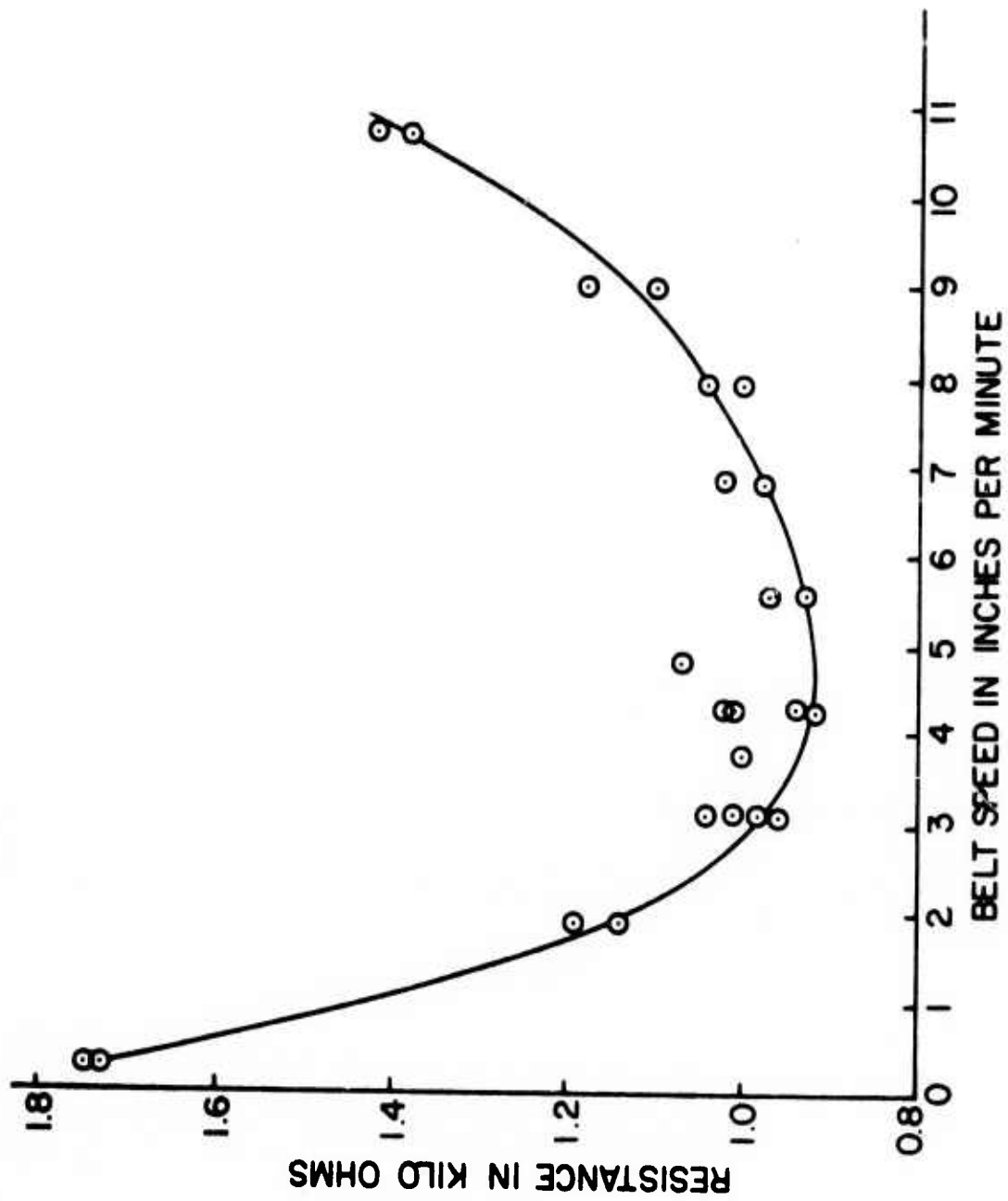


Figure 19. Resistance versus Belt Speed

on substrates with different coefficients of expansion.

#### B. End Member Pastes

In order to make the larger numbers of samples anticipated for industrial coupling and to obtain better correlation between various scientific experiments, several hundred grams of 5%  $\text{RuO}_2$  and 40%  $\text{RuO}_2$  end member pastes were formulated. Pastes with  $\text{RuO}_2$  content between these end values will be obtained by mixing appropriate quantities of the 5% and 40% pastes. Figure 20 shows the viscosity as a function of shear rate for both end members and for the 10% mix discussed earlier. These curves agree with the glass formulation defined earlier as the viscosity standard [16]. It was necessary to add a small amount of solvent to the 40%  $\text{RuO}_2$  paste after formulating with measured quantities of ingredients but it is not surprising that  $\text{RuO}_2$  powder imparts different rheological properties to the paste than the glass does. Resistance properties of the end members, i.e., blending curves, have not been determined. However, resistance versus firing was discussed in the earlier section of the report for the 10%  $\text{RuO}_2$  blend.

#### C. Comparison to Old Paste

Because of the significant difference in resistance during firing between the old and new pastes several experiments have been performed to better characterize the two pastes and their ingredients in order to determine the reason for the difference. Some difference was found in the rheological properties; the old paste had a higher viscosity that caused a thinner film to be deposited on the substrate. There was also a difference in  $\text{RuO}_2$  content of about 0.5%. These two factors could account for as much as a factor of 2 in the resistance value of the resistors made from the two pastes, but there remains a factor of 30-100. The conclusion drawn from the various experiments and observations is that most of the difference is due to a better dispersion

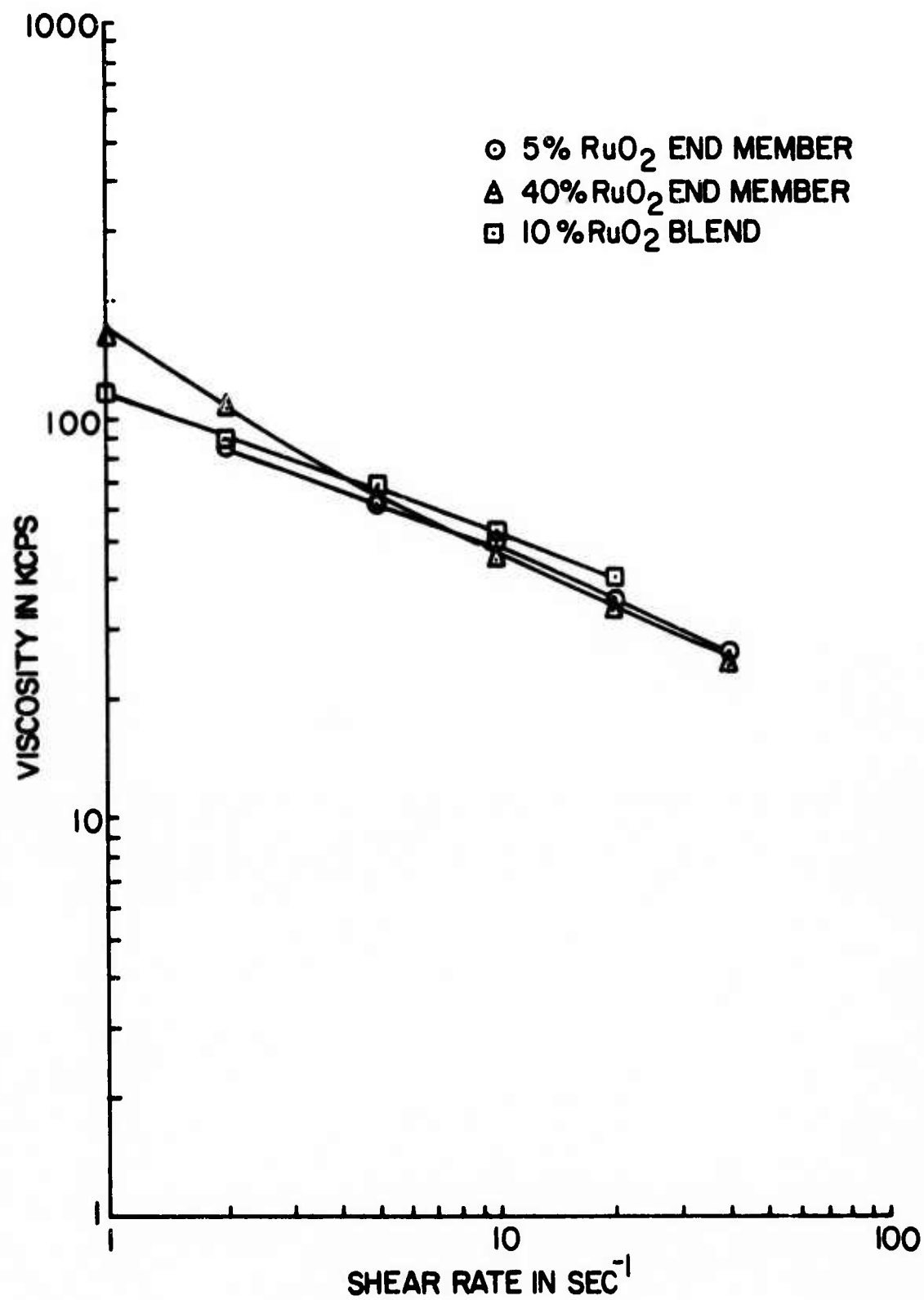


Figure 20. Rheological Properties of Resistor Pastes

of the  $\text{RuO}_2$  in the new paste and, after firing, in the glass.

The dried  $\text{RuO}_2$  powder available earlier in the laboratory and used to make the old paste is different from that obtained by drying the Englehard hydrate. [10]. X-ray line broadening studies show the Englehard powder has a smaller effective grain size, but these measurements have not been done with sufficient calibration to permit a quantitative comparison.

An Aminco Sor BET Helium carrier surface area meter was used to obtain data on the two different powders used. Both powders were prepared similarly for the BET measurement. The sample vial, into which approximately one gram of sample powder was placed, was inserted into a  $150^\circ\text{C}$  oven while being evacuated by a mechanical pump. Both samples were left in this condition for approximately seventeen hours prior to the measurement.

The calculated BET surface area was  $17.25 \text{ m}^2/\text{gram}$  for the old powder,  $1.63 \text{ m}^2/\text{gram}$  for powder used in the new paste. The surface area calculation for the old powder agrees to within a few percent of the value obtained several years ago [17], but the value for the new powder is too low. This anomaly can be explained by the fact that the BET technique actually measures the amount of nitrogen absorbed on the surface as a function of  $\text{N}_2$  partial pressure. The conclusion to be drawn from this measurement is that the two  $\text{RuO}_2$  powders have different surface characteristics. This has also been demonstrated qualitatively. If new  $\text{RuO}_2$  powder is added to water to form a suspension, the powder sinks to bottom when added to the top of the water surface, but the old powder floats and agitation is necessary to pass through the surface. SEM investigation failed to show differences in the apparent particle size or particle size distribution of the two powders.

Numerous visual examinations of resistors fired to varying stages of development have clearly indicated that the  $\text{RuO}_2$  in the new paste is better dispersed, both before and after firing. Photomicrographs obtained with transmitted light are more uniformly dark at all stages of development with the new paste as compared to light, open areas in the old paste. During high temperature firing the glass always flows slightly, causing the resistor to be larger. With the old paste the clear glass flows out beyond the portion of the resistor containing  $\text{RuO}_2$ ; with the new paste flowing glass carries the  $\text{RuO}_2$  powder with it, maintaining  $\text{RuO}_2$  dispersion. Figure 14 showed more uniform dispersion in the unfired samples of new paste, which could be due to different surface properties of the  $\text{RuO}_2$  or to different formulating techniques. In the present case both factors have probably contributed. It is common knowledge in the thick film industry that  $\text{RuO}_2$  powder obtained from different sources behave differently in resistors as well as  $\text{RuO}_2$  powder prepared by different methods from the same source.



## V. Summary and Future Plans

A coherent picture of microstructure development is beginning to emerge from studies discussed in this report; however, quantitative correlations must await completion of the sintering studies, so that the proper kinetic equations can be employed in the model. The techniques developed to arrest the microstructure development at various stages provide a powerful analytical tool for testing theoretical predictions. The possible emergence of two types of conduction mechanisms, one involving a well sintered conductive network, and the other involving contact resistance or electron transport through a glass film, may explain many of the conflicting observations and postulates made by previous workers.

The quantitative sintering studies, the measurements of resistance during firing, the microstructure investigations, and the industrial coupling, will be continued. Other studies to be continued or initiated during the coming period include:

1. Electrical Properties of the  $\text{RuO}_2$ -Glass Interface Region

Even though results reported previously indicate that the electrical properties of small particle size  $\text{RuO}_2$  are significantly different from those of massive single crystal  $\text{RuO}_2$ , the differences are not great enough to explain the nearly-zero and sometimes negative TCR observed with thick film  $\text{RuO}_2$  resistors. This phenomenon must be due to an additional effect resulting from the presence of the glass. In order to better characterize the "contact" resistance between adjacent regions of  $\text{RuO}_2$  in the glass, single crystals of  $\text{RuO}_2$  will be precoated with glass in varying thicknesses and suitable counter electrodes applied. Current-voltage measurements and capacitance

measurements as a function of bias voltage will be made in order to determine the mechanisms of charge transport through the glass films.

## 2. Particle Size Effects on the Resistivity of $\text{RuO}_2$

Previous studies on this project indicate that the apparent electrical properties of small particle size (50-100 $\text{\AA}$ )  $\text{RuO}_2$  may differ from that of the bulk, single crystal values; the electrical resistivity may be greater by a factor of about three and the TCR lower by about the same factor. A possible explanation for these phenomena is that the scattering of the conduction electrons is increased due to increased crystal defects. This increased scattering would increase the resistivity and, since defect scattering has a smaller temperature dependence than phonon scattering, the TCR would be lower. The increased scattering at the surface would be more influential with small particles and, since the smaller particles are prepared at lower temperature, there may be a higher degree of crystal disorder throughout their volume. Thus, the indications that the electrical properties of small size powder are different from those of bulk single crystal are not inconsistent with theoretical properties of materials.

The procedure for determining the resistivity of the powder will be to uniformly disperse the powder in a proper matrix, measure the resistivity of the composite, and apply the proper mixing rules. A review of heterogeneous microstructures and the associated mixing rules shows that for maximum sensitivity to the resistivity of the dispersed phase ( $\text{RuO}_2$ ), the resistivity of the matrix material should not be greater than ten times the resistivity of the powder. This excludes common dispersants since they are usually high in resistivity, and even liquid electrolytes of strong acids and bases. The only suitable materials in terms of resistivity and ease of handling are moderately low melting temperature alloys such as tin-lead solder and the

family of alloys with melting temperatures near  $100^{\circ}\text{C}$  (Wood's metal, Rose's metal, etc.). The dispersing procedure will be to melt the alloy, add the powder, and mix with a propeller while under a vacuum to avoid entrapment of air as a third phase and to minimize oxidation of the alloy.

### 3. Effects of Substrate Expansion

Substrates with coefficients of linear thermal expansion varying from 2 to  $10 \times 10^{-6}/^{\circ}\text{C}$  have been obtained and flame sprayed with a thin coating of alumina so that the resistor-substrate interface will be the same in all cases. The resistance and TCR of resistors printed and fired on these substrates will be measured and the results analyzed in light of the results obtained with the  $\text{RuO}_2$ -glass composites.

### 4. Test of Models

The sheet resistance and TCR of resistors and conductors will be determined as a function of volume fraction of conductive phase to glass, and as a function of particle size of the conducting phase and of the glass. The important glass parameters (viscosity and surface tension) will be varied at constant thermal expansion, and the results compared with predictions of the microstructure model and the interface model. Chemical additives which will alter the electrical properties according to the interface model, but which will not affect microstructure development, will be utilized to further test the interface model.

### 5. Resistor and Conductor Evaluation

Predictions of the microstructure and interface models will be utilized to develop optimum resistor and conductor formulations within the given materials system. The performance of these will be evaluated according to the list of specifications developed.

## VI. REFERENCES

1. R. W. Vest, Semi-annual Technical Report for the period 7/1/70-12/31/70, Purdue Research Foundation Grant No. DAHC-15-70-67, ARPA Order No. 1642, February 1, 1971.
2. R. W. Vest, Semi-annual Technical Report for the period 1/1/71-6/30/71, Purdue Research Foundation Grant No. DAHC-15-70-G7, ARPA Order No. 1642, August 1, 1971.
3. R. W. Vest, Semi-annual Technical Report for the period 7/1/71-12/31/71, Purdue Research Foundation Grant No. DAHC-15-70-G7, ARPA Order No. 1642, February 1, 1972.
4. R. W. Vest, Semi-annual Technical Report for the period 1/1/72-6/30/72, Purdue Research Foundation Grant No. DAHC-15-70-67, ARPA Order No. 1642, August 1, 1972.
5. R. W. Vest, Semi-annual Technical Report for the period 7/1/72-12/31/72, Purdue Research Foundation Grant No. DAHC-15-70-67, ARPA Order No. 1642, February 1, 1973.
6. Page 3, Reference 1.
7. Page 8, Reference 5.
8. Page 58, Reference 1.
9. J. Mukerji and S. R. Biswas, "Solubility of Ruthenium in Soda-Silicate Glasses," Glass and Cer. Bul. 14, 30 (1967).
10. Page 45, Reference 5.
11. Page 10, Reference 4.
12. Page 15, Reference 5.
13. Page 26, Reference 5.
14. Pages 23 and 30, Reference 2.
15. Page 20, Reference 5.
16. Page 38, Reference 3 and Page 27, Reference 4.
17. Page 44, Reference 1.